

Chemical equilibration of plasma-deposited amorphous silicon with thermally generated atomic hydrogen

Ilsin An and Y. M. Li

*Materials Research Laboratory and the Department of Physics,
The Pennsylvania State University, University Park, Pennsylvania 16802*

C. R. Wronski

*Materials Research Laboratory and the Department of Electrical and Computer Engineering,
The Pennsylvania State University, University Park, Pennsylvania 16802*

R. W. Collins

*Materials Research Laboratory and the Department of Physics,
The Pennsylvania State University, University Park, Pennsylvania 16802*

(Received 16 July 1992; revised manuscript received 5 February 1993)

Hydrogenated amorphous silicon (*a*-Si:H) thin films prepared by plasma-enhanced chemical vapor deposition (PECVD) from SiH₄ have been further hydrogenated *in situ* by exposure to atomic H generated by a filament heated in H₂ gas. Upon equilibration of the network with gas-phase H, as many as $\sim 2 \times 10^{21} \text{ cm}^{-3}$ additional Si-H bonds form within the top 200 Å of the film without significant etching, surface roughening, or coordination defect generation. Real-time spectroscopic ellipsometry is applied to study the kinetics of near-surface Si-H bond formation at 250 °C in order to improve our understanding of the effects of excess atomic H in the *a*-Si:H growth environment. Atomic H entering the film surface exhibits an effective diffusion coefficient $> 3 \times 10^{-15} \text{ cm}^2/\text{s}$ and is trapped within the top 200 Å of the film at a rate of $\sim 10^{-3} \text{ s}^{-1}$. Most of this H is trapped irreversibly on the time scale of deposition with emission rates $< 2 \times 10^{-7} \text{ s}^{-1}$. We also find that monolayer levels of surface oxide are an effective diffusion barrier to H, preventing chemical equilibration between the gas and solid phases.

I. INTRODUCTION

Recent studies of the growth, electronic properties, and stability of hydrogenated amorphous silicon (*a*-Si:H) thin films prepared by plasma-enhanced chemical vapor deposition (PECVD) from SiH₄ have concentrated on the ability of excess atomic hydrogen in the growth environment to alter the chemical equilibrium between Si-Si and Si-H bonds in the network.¹⁻³ It has been suggested that an increase in the H chemical potential in the solid can passivate weak Si-Si bonds, thereby increasing the network order and its stability against light-induced defect generation. This may be accomplished during growth by increasing the H chemical potential in the gas phase, as long as equilibrium between the gas phase and solid can be ensured.³ Initial studies show that approaches involving excess atomic H in the *a*-Si:H growth process are promising and material improvements have been reported.^{1,2}

An understanding of such processes is limited by available kinetic information on hydrogen diffusion and reaction in the near surface of *a*-Si:H in the growth environment. For example, Street has proposed an equilibration zone at the growing film surface of thickness $d_{\text{eq}} \sim D/r$, where D is the hydrogen diffusion coefficient and r is the *a*-Si:H deposition rate.³ If the deposition rate is too high relative to the diffusion rate, this zone collapses and the solid chemical potential cannot equilibrate with

that in the gas. Reliable information on diffusion typically comes from secondary ion mass spectrometry (SIMS) studies of annealed multilayers having deuterated/hydrogenated *a*-Si components.⁴⁻⁶ In the growth environment, however, the initial conditions are different, namely, H is in a mobile state upon injection at the *a*-Si:H surface, and diffusion is driven by the chemical potential difference. Thus it is not clear that such determinations of the diffusion coefficient are relevant for assessing equilibration during growth.⁷ In fact, H (or deuterium D) diffusion in *a*-Si:H has been found to be faster when the H (or D) is introduced from a plasma at the surface in comparison to when it originates internally from the solid.^{8,9} Very recently such effects have been discussed in terms of a concentration-dependent diffusion coefficient.¹⁰

Optimum development of growth techniques that involve gas/solid phase H equilibration is limited by the availability of sensitive probes that can characterize near-surface microstructural changes. It has been proposed that at a sufficiently high H chemical potential at the film surface, for example, etching reactions dominate and microcrystalline Si domains form at the surface that may be detrimental to the material properties in device applications.^{3,11} Thus one may seek to raise the chemical potential to a level just below the critical threshold for microcrystallite formation, but this would be very difficult in the absence of real-time feedback. In addition,

growth/equilibration techniques that involve excess gas-phase atomic H must avoid potentially damaging effects due to direct H plasma exposure.

In this paper, we describe an alternative technique for *in situ* hydrogenation of *a*-Si:H that involves exposing the film to atomic H, thermally generated with a filament. There are two important aspects to this approach. First, the filament process avoids energetic particle impact at the *a*-Si:H surface. Second, the process can be used *in situ* in conjunction with conventional PECVD *a*-Si:H to prepare H-modified materials. By alternating *a*-Si:H growth with *in situ* exposure to thermally generated H at the substrate temperature of $\sim 250^\circ\text{C}$, materials can be prepared with uniformly elevated H chemical potentials that can be frozen in upon cooling the samples. The properties of such materials can then be compared to those of continuously grown materials for a direct comparison of the effects of network equilibration on properties and stability. Such efforts are discussed in detail elsewhere.¹² Here, we will present a real-time spectroscopic ellipsometry (SE) study of the kinetics of H trapping (Si-H bond formation) and emission (Si-H bond breaking) that result from exposing PECVD *a*-Si:H to thermally generated atomic H at $\sim 250^\circ\text{C}$, the optimum temperature for deposition. These results provide insights into the effects of excess gas-phase atomic H in the growth environment on subsurface bonding in *a*-Si:H.

II. EXPERIMENTAL DETAILS

The *a*-Si:H films were prepared by parallel-plate rf PECVD in a turbopumped, UHV-compatible chamber with the following parameters: pure SiH_4 pressure, 0.2 Torr; SiH_4 flow, 20 standard cm^3/min ; rf plasma power, 52 mW/cm^2 ; and substrate temperature, 250°C . Under these conditions, the deposition rate is $1.4 \text{ \AA}/\text{s}$. Silicon wafer substrates were used for optical studies because of their smoothness. Atomic H treatments of *a*-Si:H were performed *in situ*, i.e., with the sample mounted in the same configuration as for growth, at nominally the same substrate temperature. The substrate temperature decreases in the initial stage of treatment as a result of thermal losses due to the introduction of H_2 , but it can be held typically to within $\sim 10^\circ\text{C}$ of the initial value. Power levels of 20–35 W were applied to a W filament 5 cm long and 0.025 cm in diameter in order to generate the atomic H from 8 mTorr H_2 gas. The highest power provides an approximate filament temperature of 2250°C .

For high-resolution SIMS studies of diffusion, the filament was ignited in pure D_2 gas for deuteration. The D treated films were capped for protection by an additional PECVD *a*-Si:H layer, and the original position of the surface was identified in the SIMS profile by small spikes of O, C, and N impurities that are introduced in the D treatment. In a study of *a*-Si:H treated by atomic D at low temperature, we estimate a SIMS resolution of at least 50 Å per order of magnitude decrease in D concentration.

Optical access to the sample surface during *a*-Si:H growth and H treatment is provided by windows at a 70° incidence angle. Real-time SE measurements were per-

formed over the range from 2.5 to 4.5 eV with a multichannel rotating polarizer ellipsometer as described elsewhere.¹³ This spectral range provides optical penetration depths (OPD's) from 500 to 50 Å for *a*-Si:H at 250°C . Full spectra in the ellipsometric parameters (ψ, Δ) were collected every 1 to 15 s, depending on the desired time resolution. Here, $\tan\psi \exp(i\Delta) = r_p/r_s$, where r_p and r_s are the complex amplitude reflection coefficients of the surface for linear *p*- and *s*-polarization states. In this study, we focus on the equilibration of the top 200 Å of the *a*-Si:H that occurs upon H treatment. Real-time SE experiments suggest that under optimum PECVD conditions, the near surface of the film prior to H treatment is representative of the bulk, with the possible exception of the topmost $\sim 10 \text{ Å}$.¹⁴

III. RESULTS AND ANALYSIS

First, the effects of H treatment on the optoelectronic properties of optimum *a*-Si:H will be reviewed.¹² Thick films ($> 5000 \text{ Å}$) were prepared by alternating growth and heated-filament H treatment to achieve uniform equilibration throughout the film thickness, using procedures developed in our real-time SE study. Such films have been measured using infrared transmittance and dual beam photoconductivity techniques. The results show that as many as $2 \times 10^{21} \text{ cm}^{-3}$ (4 at. %) additional H atoms can be incorporated in Si-H bonds, depending on the conditions of treatment, but without generating coordination defects at the level of 10^{15} cm^{-3} that lead to excess absorption in the 0.8–1.2 eV range. More than 80% of the additional incorporated H exhibits an infrared stretching mode at 2000 cm^{-1} , while the remainder exhibits 2090 cm^{-1} . On the basis of these results, we can interpret the real-time SE data simply in terms of the conversion of Si-Si to Si-H bonds.

A. Dielectric response of the introduced Si-H bonds

The initial goal of our experiments is to obtain an approximate measure of the near-uv dielectric response of the Si-H bonds introduced by the H treatment, for use in kinetic analyses. First, an *a*-Si:H film was grown to opacity (for energies $> 2.5 \text{ eV}$) and monitored in real time by SE. The real-time SE analysis of Ref. 14 provided the microscopic roughness layer thickness on the film surface as well as the true dielectric function of the bulk *a*-Si:H, shown in Fig. 1. Next, a 1-h atomic H treatment of the *a*-Si:H was performed and monitored by real-time SE. By this time, complete saturation of the optical modification has occurred, and the SE data remain unchanged with further exposure. By subsequent inspection of the SE data, namely, the $\Delta(h\nu)$ spectra, we verified that the roughness layer remained unchanged in thickness during this H treatment. As a result, the *a*-Si:H dielectric function after treatment could be obtained without further information (see Fig. 1). This latter result is only strictly valid, however, if the additional H is incorporated uniformly throughout the OPD so that there is no gradient in the optical properties with probing depth. This is true at least to a depth of $\sim 200 \text{ Å}$, as

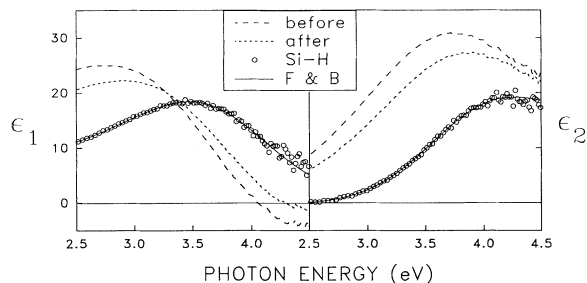


FIG. 1. Real and imaginary parts of the dielectric function of *a*-Si:H deduced from real-time (ψ, Δ) spectra collected before and after a 1-h atomic H exposure of *a*-Si:H at 250°C (broken lines). The dielectric response of the modified Si-H bond component deduced from these two spectra is also shown (points). The solid line is a fit to the latter using the Forouhi-Bloomer model of the dielectric response of an amorphous semiconductor.

demonstrated from SIMS studies using atomic deuterium (D) treatment. (See the inset of Fig. 3 and Fig. 5 for the relevant profile obtained with a 1-h treatment.) Thus the dielectric function after H treatment should be valid at energies > 2.9 eV, where the OPD is < 200 Å.

One clear effect of the H treatment on the dielectric function, as shown in Fig. 1, is a reduction in the overall magnitude of ϵ_2 . Based on this observation, the simplest possible optical interpretation applies the assumption that single Si-Si bonds are the fundamental polarizable units and Si-H bonds do not contribute to the polarizability.¹⁵ Thus the conversion of Si-Si bonds to Si-H bonds can be represented solely in terms of the formation of void volume. With this model, the 1-h H treatment is consistent with the conversion of 7 vol % of the original material into voids, as estimated from the Bruggeman effective-medium theory (EMT) and linear regression analysis (LRA). However, the fit to the modified dielectric function in Fig. 1 using the simple void incorporation model is poor since such a model cannot explain the observed shift to higher energy in the ϵ_2 peak that occurs with H treatment.

In a second modeling attempt, we have used the approach of Mui and Smith¹⁶ who assumed that the basic polarizable units are $\text{Si-Si}_{4-n}\text{H}_n$ ($n=0, \dots, 3$) tetrahedra. Thus we have assumed that some volume fraction of Si-Si₄ units are converted to Si-Si₃H units upon H treatment, and we have proceeded to fit the modified dielectric function in Fig. 1 using a three-component composite of (i) original material, (ii) Si-Si₃H volume, and (iii) void volume. The dielectric function of the Si-Si₃H tetrahedron is obtained by scaling the dielectric function of *a*-Si:H at 250°C, using the theoretical approach discussed in detail in Ref. 16. (Data for *a*-Si:H at the elevated temperature are required since the results of Fig. 1 are characteristic of the substrate temperature of 250°C.) In the fitting procedure, we fix the volume fraction associated with the Si-Si₃H component at ~ 0.04 . This value is derived from the relationship between volume fraction

and atomic percent established by the tetrahedral volumes used in Ref. 16, along with the ~ 4 at. % estimate for the additional Si-H bonds deduced from infrared spectroscopy. Unfortunately, we found that the best fit to the modified dielectric function in Fig. 1, having ~ 4 vol % Si-Si₃H and ~ 6 vol % void, is only slightly improved over the simpler void incorporation model described above. An inspection of the experimental and best fit dielectric functions again shows a clear disagreement in the peak energy. This problem cannot be resolved by allowing possible errors of 50% in the infrared determination of the additional H concentration (which would lead to a possible Si-Si₃H volume in the range 2–6 vol %). The possible sources of error associated with the tetrahedron model may include invalid assumptions concerning (i) the dielectric function of the Si-Si₃H units and (ii) the optically affected volume per incorporated H atom.

The problem with the void incorporation and tetrahedron models is further emphasized by a more sensitive, yet general, analysis procedure. In this procedure, we make only one assumption, namely, that some volume fraction of the *a*-Si:H is converted upon H treatment to an “unknown” material with the dielectric response of the additional Si-H bond and void volumes that may be formed. The dielectric response of the unknown material can be determined from the EMT and the dielectric functions before and after H treatment, but only if the volume fraction f_0 is known. If f_0 is chosen to be equal to either of the two total volume fractions from the void and tetrahedron models, 0.07 and 0.10, then the resulting unknown materials exhibit dielectric functions with ϵ_2 values that drop below 0 for $h\nu < 3.2$ eV. This behavior demonstrates that the two models are inappropriate. It is only when f_0 is increased to 0.24 that the deduced ϵ_2 exhibits positive values for $h\nu < 3.2$ eV and smoothly approaches zero for $h\nu < 3.0$ eV. We call the resulting material the “Si-H bond component” (in spite of the fact that void volume may also be included).

Figure 1 includes the results for the dielectric function of the Si-H bond component (points) deduced with $f_0=0.24$. Also shown in Fig. 1 is a fit to these spectra using a general description of the dielectric function of an amorphous semiconductor, developed by Forouhi and Bloomer (FB), which satisfies Kramers-Kronig (KK) relations.¹⁷ The excellent fit shows that $f_0=0.24$ is the minimum value for the volume fraction that leads to a Si-H component dielectric function satisfying KK relations. For this reason, we use it along with the EMT and LRA for all kinetic analyses of the real-time SE data.

It is surprising that, in a number of studies such as these, we find a volume fraction for the Si-H bond component that is always three to five times the additional atomic percentage of H deduced from infrared spectroscopy. (The range here is associated with uncertainties in the determination of differences between the H content of samples measured by the infrared technique.) We need to consider this observation in greater detail. First, the Si-H bond component dielectric response in Fig. 1 may include some void volume as a result of network relaxation in the modified material. Based on electron density considera-

tions, however, we estimate that this is no more than 30% of the total Si-H component volume. As a result, we conclude that the radius of the spherical volume that is optically affected by a single incorporated H atom is not 1.6 Å as in the tetrahedron model,¹⁶ but is in the range 2.3–2.6 Å.

The implications of this result are not fully understood at present and further research is required. However, any such investigations are beyond the scope of the present study that focuses on the kinetic behavior of the Si-H bond component (assumed to be proportional to the additional bonded H content). In fact, the same kinetic behavior is observed within $\sim \pm 15\%$, irrespective of the choice of optical model from among the three discussed above; only the absolute volume fraction normalization is very sensitive to the optical model. Since the basic conclusions of this paper depend only on the kinetic information, their validity does not rest on the optical model.

B. Modification and etching of *a*-Si:H by atomic H

Figure 2 shows an example of the practical capabilities of SE, once the optical response of the Si-H bond component is known. In this experiment, (ψ, Δ) spectra were collected in real time during *in situ* exposure of freshly deposited 150-Å-thick *a*-Si:H to atomic H under different filament conditions. The film was maintained near its deposition temperature of 250°C. The spectra have been interpreted by LRA to extract the two photon energy-independent parameters of film thickness and volume fraction of the Si-H bond component incorporated during treatment. The latter must be considered an average throughout the thickness of the film since uniformity in

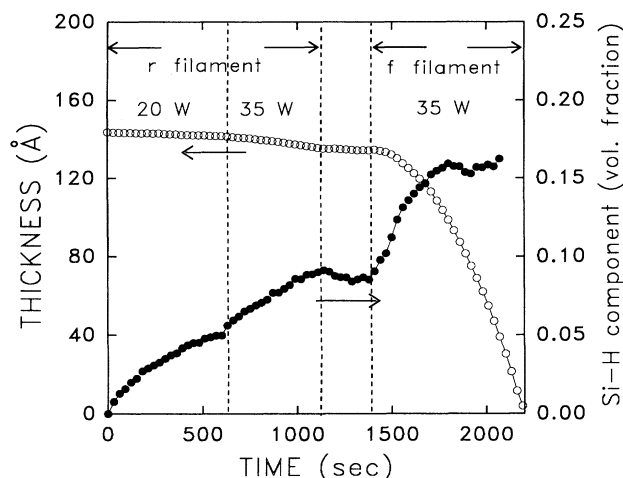


FIG. 2. Time evolution of film thickness (open points) and Si-H bond component volume fraction (solid points) deduced from real-time SE data collected as 150-Å-thick, optimum PECVD *a*-Si:H at 250°C is exposed to thermally generated atomic H. Initially a rear (*r*) filament that lacks direct line of sight to the sample surface is ignited at 20 W. The power applied to the filament is increased to 35 W after ~ 10 min. After another ~ 8 min, this filament is extinguished, and a front (*f*) filament with a line of sight to the sample is ignited.

the Si-H component cannot be ensured for this shorter time scale (< 20 min). The use of a very thin film in this example tends to minimize such a problem, however.

In Fig. 2 at $t=0$, a rear filament without direct line of sight to the sample surface is ignited with 20 W, and at $t \sim 10$ min the power is increased to 35 W. At $t \sim 18$ min the rear filament is extinguished, and a few minutes later a second filament with direct line of sight to the sample is ignited with 35 W. With this front filament, the Si-H component volume fraction increases more abruptly and stabilizes at ~ 0.15 as relatively rapid etching (average rate -0.17 Å/s) commences. For a given filament power, the etch rate is more than an order of magnitude lower for the rear filament (-0.012 Å/s), an indication of a lower flux of H at the film surface, and possibly an absence of direct electron impact. At 20 W filament power, only ~ 12 Å of *a*-Si:H are removed in a 1-h treatment (-0.0035 Å/s).

C. Kinetics of H trapping in *a*-Si:H

As can be inferred from the example of Fig. 2, the true advantage of SE is the continuous kinetic information it provides; however, depth profiling with ellipsometry is problematic. Thus SE is complementary to SIMS. For thicker films (> 200 Å), we concentrate on modeling SE data only over the higher photon energy range, $2.9 \leq h\nu \leq 4.5$ eV, in order to reduce the maximum OPD to less than 200 Å, and hence, to minimize the degree of depth averaging that is incurred. One difference between the SE and SIMS techniques originates from the fact that SE detects only the additional H atoms that bond to Si as a result of the treatment and is insensitive to the presence of any trapped H₂ or unbonded H. Over the time scale of interest, however, the unbonded H is probably a much smaller fraction of the total incorporated H owing to its anticipated short lifetime in the *a*-Si:H network. The sensitivity of the SE technique to different sites for H will be discussed in greater detail when the experimental results are interpreted.

The inset in Fig. 3 shows high-resolution SIMS deuterium depth profiles of the *a*-Si:H film for 20- and 60-min atomic D treatments at 240°C using a rear filament (solid lines). In this type of plot, we focus on the high concentration, near-surface region in order to emphasize the features relevant to SE which is a linear, surface-sensitive probe. Because the extrapolated surface concentration in the inset of Fig. 3 increases with time, we note that the observed profiles cannot strictly obey the functional relationship expected for diffusion-limited incorporation of mobile deuterium, namely, $C(x, t) = C_0 \operatorname{erfc}[x / (4Dt)^{1/2}]$. In fact, the time dependence of the profile in the top 200 Å in Fig. 3 appears to be dominated by a time-dependent, multiplicative prefactor, meaning that $C(x, t)$ can be approximated as a separable function of x and t . Thus even the shapes of the SIMS profiles do not follow the complementary error function (erfc). This is demonstrated by the broken lines, calculated from the erfc relationship by fixing C_0 at the experimentally observed near-surface values and setting $D = 2.8 \times 10^{-14}$ cm²/s, which provides the best agreement to the top 200 Å of the two observed

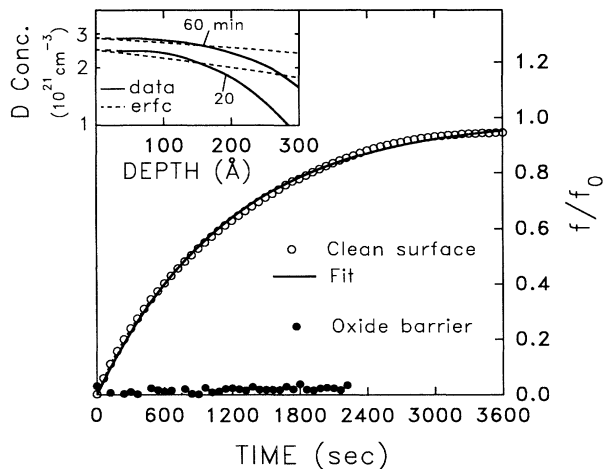


FIG. 3. Volume fraction of Si-H bond component, f , normalized to the ultimate saturation value, f_0 , deduced from real-time SE data collected as a function of time during atomic H treatment of 2500-Å-thick, optimum PECVD a -Si:H at 250°C. For the open points the treatment is performed *in situ* upon terminating the deposition. For the solid points, the a -Si:H was exposed to air (at 250°C) prior to H treatment. The solid line was obtained as the best fit to the former using an expression of the form $f = f_0[1 - \exp(-at)]$. The inset shows typical deuterium depth profiles from SIMS in the top 300 Å of the film for 20 min (lower curve) and 60 min (upper curve) D treatments at 240°C. The broken lines are fits to the SIMS results in the top 200 Å using a complementary error function profile with the prefactor fixed at the observed surface concentration ($x=0$).

profiles. A comparison between the experimental and calculated profiles shows that the former exhibit a step-like behavior that can be understood using a model of trap-dominated diffusion, to be described in greater detail shortly.¹⁸

We find that the evolution of the SE (ψ, Δ) spectra during H treatment is also inconsistent with the development of a simple diffusion-limited depth profile for the additional concentration of H bonded to Si. Again, by confining the ellipsometric analysis to photon energies with OPD's < 200 Å, excellent fits to the evolution of the SE spectra are obtained assuming that the Si-H bond component evolves according to $C(x,t) = T(t)$, meaning that the bonds form nearly uniformly throughout the OPD. The discussion below (see Fig. 4) will provide further quantitative justification for this interpretation. At this point we simply state that SE can provide experimental values proportional to the additional concentration of bonded H within the top 200 Å of the film, continuously versus time during H treatment. Such information is not accessible by any other currently available characterization technique.

Figure 3 shows a plot of $f(t)/f_0$, where f is the additional volume fraction of the incorporated Si-H bond component and f_0 is its saturation value, obtained in a LRA of SE data collected during H treatment of a 2500-Å-thick film using a rear filament at 28 W. The fit to the

data (solid line) shows that $f(t)$ exhibits exponential kinetics, i.e.,

$$f(t)/f_0 = 1 - \exp(-at), \quad (1)$$

with a best fit single "reaction" rate of $\alpha = 8 \times 10^{-4} \text{ s}^{-1}$. The remaining deviation in Fig. 3 between the data and the fit can be attributed to a second, much smaller ($\sim 0.07f_0$) contribution to the Si-H bond component with a higher rate of $5 \times 10^{-3} \text{ s}^{-1}$. Since a similarly high rate is dominant in films prepared under conditions that lead to a high void volume fraction (e.g., a high Ar:SiH₄ gas dilution ratio), it is possible that this contribution arises from a second reaction site for H associated with void or weak-bond channels.

In order to understand the behavior of Eq. (1), let us now consider H transport via trap-dominated diffusion.¹⁸ Suppose that mobile H diffuses via continuous interaction with shallow traps, whereas when it is captured by a deep trap, it is immobilized for at least as long as the minimum detectable time increment in the measurement ($t_d \sim 10 \text{ s}$ in Fig. 3). By defining ΔE as the binding energy for H at

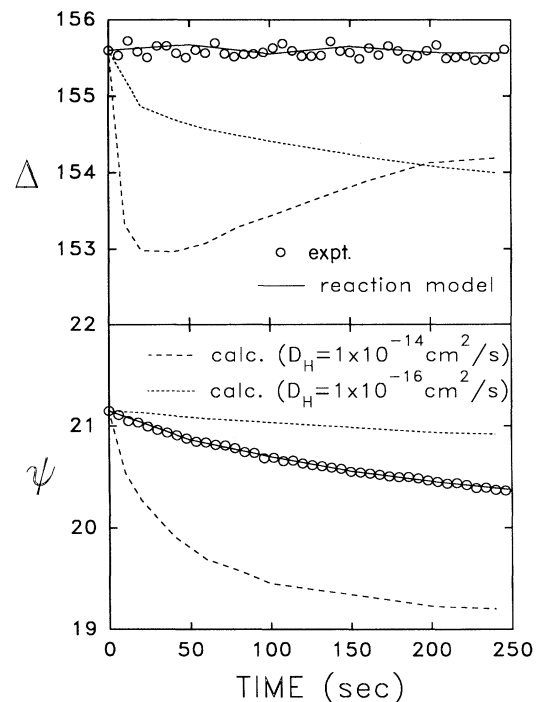
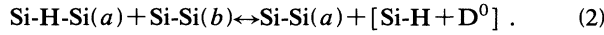


FIG. 4. Experimental ellipsometric angles (ψ, Δ) in degrees, at a photon energy of 3.0 eV collected vs time at ~ 1 -s intervals during H treatment of a -Si:H at 250°C, under the same filament conditions as in Fig. 3 (only every sixth data point is plotted for clarity). The broken lines show the results of simulations calculated from complementary error function profiles assuming identical surface concentrations of mobile H and diffusion coefficients of 10^{-16} and $10^{-14} \text{ cm}^2/\text{s}$. Faster diffusion leads to an abrupt change in Δ as the diffusion front moves within the window of observation, which is the optical penetration depth (OPD) in a -Si:H at 3.0 eV and 250°C ($\sim 175 \text{ Å}$). The solid line shows the expected behavior for the incorporation of H uniformly throughout the OPD according to Eq. (1).

a trapping site (i.e., the energy required for H emission), then $\Delta E_d = kT \ln(\alpha_{e0} t_d)$ defines the binding energy that demarcates shallow and deep traps in a continuous distribution. In this expression, α_{e0} is the attempt frequency for H emission. For the time scale of the experiment of Fig. 3 and an assumed attempt frequency of $10^{12} - 10^{13} \text{ s}^{-1}$, we estimate that a deep trap has a H binding energy $> 1.40 \pm 0.05 \text{ eV}$.

The following reaction represents one of a number of the simplest possible diffusion and deep-trapping processes proposed in earlier studies:⁵



Here (a) represents a shallow trap, e.g., a bond-center site, through which H transport can occur, and (b) represents a deep trap where structural relaxation is possible that generates a Si-H bond and a Si dangling bond (D^0). More recent research suggests that H trapping in complexes may be more likely, for example, two interstitial H atoms that associate to form a H_2^* , a bond-center H with an adjacent H in a tetrahedral interstitial site.¹⁹

When a single type of deep trap is dominant, then we can express the concentrations C_t of deep-trapped H and C_m of mobile (free and shallow-trapped) H with the following equations:¹⁸

$$\frac{\partial C_t}{\partial t} = \alpha_c C_m (C_{t0} - C_t) - \alpha_e C_t, \quad (3)$$

$$\frac{\partial C_m}{\partial t} = D_m \left[\frac{\partial^2 C_m}{\partial x^2} \right] - \alpha_c C_m (C_{t0} - C_t) + \alpha_e C_t, \quad (4)$$

where C_{t0} is the total concentration of deep traps available at the elevated H chemical potential. In Eqs. (3) and (4), $\alpha_c = 4\pi D_m r_c$ and $\alpha_e = \alpha_{e0} \exp(-\Delta E/kT)$ are the rate coefficients for H capture by and emission from the deep traps, respectively, where r_c is the capture radius and D_m is the effective diffusion coefficient of the H. Because H transport is controlled by capture and emission from the shallow traps, D_m is a function of the distribution of H within the shallow traps and therefore may in general depend on the depth (i.e., H concentration) and time.^{10,20}

We will show later that the dominant deep traps for H are irreversible on the time scale of interest, so that the last terms on the right in Eqs. (3) and (4) can be neglected. The solution to Eq. (3) is

$$C_t(x, t)/C_{t0} = \{1 - \exp[-\alpha_c \langle C_m(x, t) \rangle t]\}, \quad (5)$$

where

$$\langle C_m(x, t) \rangle = t^{-1} \int_0^t C_m(x, t') dt' \quad (6)$$

is the average of the mobile H concentration over time t . Shortly, we will also argue that the optical contribution to the Si-H bond component in Fig. 3 from mobile H is much smaller than that from deep-trapped H. Then we can associate f/f_0 in Eq. (1) with C_t/C_{t0} in Eq. (5). Thus, in order to maintain consistency with observations leading to Eq. (1), C_m in Eq. (6) must be nearly independent of t [except possibly when $t \ll (\alpha_c \langle C_m \rangle)^{-1}$; see Eq. (7)]. Because the SIMS profile is also dominated by C_t

and is reasonably constant within the top 200 Å of the film, at least for $t > 1.2 \times 10^3 \text{ s}$, then C_m on the right in Eq. (6) must also be nearly independent of x .

The combined results simply mean that the diffusion rate of H through the top 200 Å is much faster than the dominant deep-trapping rate, and C_m has saturated at its near-surface value, C_{m0} , established by the atomic H flux. Using the combined results we can express the rate coefficient in Eq. (1) as $\alpha = \alpha_c C_{m0} = 8 \times 10^{-4} \text{ s}^{-1}$. Faster diffusion in comparison to deep trapping means that $D_m > \alpha_c C_{m0} x_{\text{max}}^2 = 3 \times 10^{-15} \text{ cm}^2/\text{s}$, where x_{max} is the maximum depth under consideration, 200 Å. Thus a much higher diffusion coefficient is estimated for H initially injected into mobile states at the film surface, in comparison to measurements in which the diffusing H is initially deep trapped.

Next, we consider the possible contribution of mobile H to the SE results (f/f_0) at short times in Fig. 3. In the limit where $t \ll (\alpha_c C_{m0})^{-1}$ (or $t < 200 \text{ s}$), $C_t \ll C_{t0}$ and Eq. (4) can be solved easily. The result is

$$C_m(x, t) = C_{m0} \exp(-\alpha_c C_{t0} t) \text{erfc}[x/(4D_m t)^{1/2}]. \quad (7)$$

First if $C_{m0} \geq C_{t0}$, then the exponential factor can be set to unity. In addition, if the mobile H generates a change in dielectric response similar to that of the immobilized H, then the SE data should be dominated by a diffusion-limited profile in C_m at short times as long as $D_m > 1 \times 10^{-17} \text{ cm}^2/\text{s}$. Diffusion-limited profiles are detectable by SE even as they penetrate the top few Å of the film, as a result of the sensitivity of the Δ spectrum to surface layers of different optical properties.

For the experiment of Fig. 4 (points), the angles (ψ, Δ) at a photon energy of 3.0 eV were collected versus time at 1-s intervals during a ~ 250 -s H treatment of *a*-Si:H at 250°C. Simulated results assuming $C_{m0} = C_{t0}$ and diffusion coefficients of 10^{-16} and $10^{-14} \text{ cm}^2/\text{s}$ were calculated from complementary error function depth profiles and multilayer optical analysis (broken lines). The absence of a shift in the experimental Δ value indicates that a diffusion-limited profile of Eq. (7) is inconsistent with the data even for the shortest times. This in turn forces us to conclude that either the mobile concentration of H is too low to be detected or the optical change that it induces in the network is too weak. From a quantitative sensitivity analysis, we conclude that $(C_{m0}/C_{t0}) \equiv R < 0.1$ if the dielectric response of the H introduced in the mobile state is similar to that of the deep-trapped H. In fact, R could be larger than 0.1, but only if the optical effect of the mobile H is weaker than that of deep-trapped H, e.g., if the dielectric response associated with the mobile H is closer to the unmodified dielectric function than to the response of the Si-H bond component given in Fig. 1 (points). The solid lines in Fig. 4 that match the experimental results have been calculated assuming a buildup of the Si-H bond component uniformly throughout the penetration depth of the light according to the form of Eq. (1). This suggests that the effective diffusion coefficient for these short times is as much as an order of magnitude larger (i.e., $D_m > 4 \times 10^{-14} \text{ cm}^2/\text{s}$) than that estimated earlier from

the longer time behavior.

It is now instructive to return to a more detailed inspection of the SIMS deuterium profile, assuming that it represents the distribution of deep-trapped H, $C_i(x, t)$. Figure 5 shows the D profile obtained after 1 h of treatment, from the inset of Fig. 3, but plotted over wider depth and concentration scales. Because the deep-trapping process has nearly saturated after one hour ($t \sim 3\alpha^{-1}$), we can apply an approximate solution to Eqs. (3) and (4) from Ref. 18 in order to extract more information on the diffusion process from an inspection of the observed profile. The effective diffusion coefficient of the mobile H in Eq. (4) can be estimated from three features of this depth profile, namely, (i) x_c , the depth at which the concentration drops by a factor of 2; (ii) δx , the width of the profile, i.e., the inverse linear slope at the depth x_c ; and (iii) κ , the exponential slope of the fall off in the profile. The following three simple relationships hold:

$$D_m = \frac{x_c^2}{4Z_c^2 t} \quad (8a)$$

$$= \frac{(\delta x)^2 \alpha Z_c^2}{R} \quad (8b)$$

$$= \frac{\alpha}{\kappa^2 R}, \quad (8c)$$

where Z_c depends only on the ratio $R \equiv C_{m0}/C_{i0}$ and is the solution to the equation:¹⁸

$$Z_c \exp(Z_c^2) [1 - \operatorname{erfc}(Z_c)] = \pi^{-1/2} R. \quad (8d)$$

Using the values from Fig. 5 for x_c , δx , and κ^{-1} of 320, 160, and 40 Å, respectively, we find the best agreement in D_m for the three expressions of Eqs. (8) when $R \sim 0.2$.

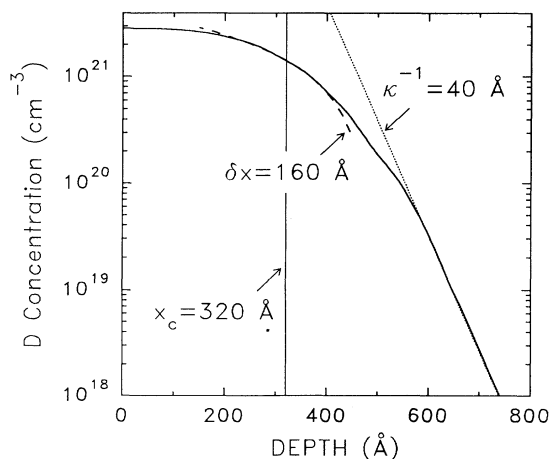


FIG. 5. Deuterium depth profile from SIMS for a 1-h exposure of *a*-Si:H to atomic D, reproduced from the inset of Fig. 3 over a wider depth and concentration range. Three parameters can be extracted from the profile in order to obtain information on trapping and diffusion. x_c is the depth at which the profile drops by a factor of 2 from its near-surface value; δx is the width of the profile, i.e., the inverse linear slope at a depth x_c ; and κ is the exponential slope of the D tail deep into the sample.

The agreement in D_m , however, can be achieved only to within about one order of magnitude for the three expressions. The largest value of D_m , 7×10^{-15} cm²/s, is obtained from x_c , i.e., the part of the profile closer to the surface. The smallest value, 8×10^{-16} cm²/s, is obtained from the exponential fall off deeper into the bulk of the sample. Such a range in the effective diffusion coefficient is plausible, given the dispersive nature and possible concentration dependence of the H transport process.¹⁰ It should also be noted that if the near-surface concentration of mobile H (or R) is overestimated, then D_m is underestimated.

The effective diffusion coefficient estimated from the 1-h SIMS profile at a depth of 300 Å is within the limits established by the observed deep-trap-dominated kinetics in the real-time SE data. However, for H within the penetration depth of the light (200 Å) and for shorter times, D_m may be even larger, based on arguments given earlier. In addition, a near-surface value of the concentration of mobile H given from the SIMS profile by $C_{m0} = 0.2C_{i0}$ would result in a detectable diffusion-limited characteristic at short times in Fig. 4. The fact that such a characteristic is not observed indicates that when H occupies mobile sites, a weaker optical effect occurs in comparison to when H occupies deep traps. This would be consistent with mobile configurations that do not fully disrupt the Si-Si bonding, thereby leading to a smaller change in the local polarizability of the site.

By combining Eq. (8c) with the expression $\alpha = 4\pi C_{m0} D_m r_c$, and using the deep-trap density of $C_{i0} = 2 \times 10^{21}$ cm⁻³ inferred from infrared transmission measurements, the effective capture radius of the deep traps can be estimated from the exponential slope in the SIMS profile of Fig. 5. The result, $r_c \sim 0.025$ Å, is smaller than would be expected based on the size of the Si-Si bond ($\sim 1-2$ Å). There are a number of possible explanations for this result, including the existence of a barrier to deep trapping.

D. Kinetics of H emission in *a*-Si:H

In order to separate trapping and emission and show that $\alpha_e \ll \alpha = \alpha_c C_{m0}$, as was assumed earlier in solving Eqs. (3) and (4), we propose that upon extinguishing the filament $C_{m0} \rightarrow 0$. Then the evolution of the observed Si-H bond component provides direct information on α_e . Figure 6 shows the decay in the Si-H component upon extinguishing the filament at $t = 0$ after exposing a freshly deposited 4000-Å-thick *a*-Si:H film to a 30-min H treatment. The sample temperature was maintained near 250 °C throughout growth, treatment, and the H-emission measurement. Data collection in Fig. 6 extends over a period of one hour, however, additional data were also collected over a 10-h period, 9 h later. A fit to the data in the first hour in Fig. 6 (solid line), using an activated emission law, yields two discrete rate coefficients, 4×10^{-3} and 4×10^{-4} s⁻¹ that suggest trap depths of $\sim 1.55 \pm 0.05$ and $\sim 1.65 \pm 0.05$ eV, if we were to assume an attempt frequency in the range $10^{12} - 10^{13}$ s⁻¹. The associated traps account for approximately 0.6 and 1.2 vol % out of a total of 11 vol % Si-H component intro-

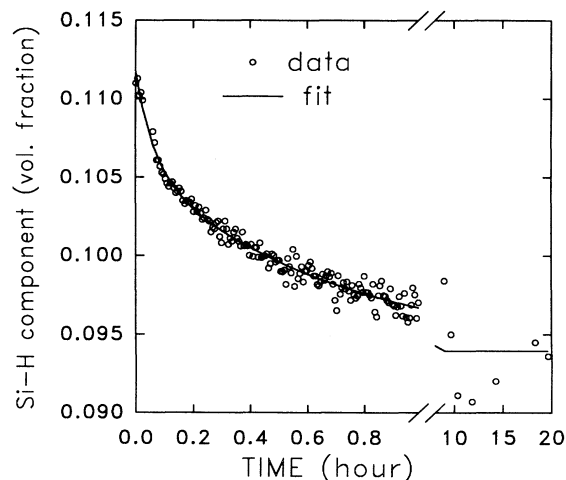


FIG. 6. Time evolution of the Si-H component in the top 200 Å of optimum PECVD *a*-Si:H at 250°C obtained from an analysis of real-time SE data collected after terminating the atomic H treatment at $t=0$. Prior to extinguishing the filament, the 4000-Å film was exposed to atomic H for 30 min. SE data were collected continuously in the first full hour after terminating treatment, and at selected times for $9 < t < 20$ h. The solid line in both regimes is the best fit to an emission rate law, $f = f_{01} \exp(-\alpha_{e1}t) + f_{02} \exp(-\alpha_{e2}t) + f_{03}$, assuming three types of traps, the third with an emission rate $< 2 \times 10^{-7} \text{ s}^{-1}$.

duced in the original H treatment. The dominant contribution to C_t , 9.5 vol % (or 85% of the total bonded H incorporated in the H treatment), exhibits emission rates less than $2 \times 10^{-7} \text{ s}^{-1}$, as can be seen by comparing the data after 10–20 h to the extrapolation of the fit (see Fig. 6 at right). This suggests that the dominant traps have a depth of more than 2.0 eV. The overall analysis justifies the earlier assumption and demonstrates that the dominant H-emission rates are several orders of magnitude lower than the capture rate, and the buildup of the Si-H component in Fig. 3 reflects predominantly capture processes.

E. Effects of surface bonding on the modification of *a*-Si:H by atomic H

In all measurements reported so far, the H treatment was performed *in situ* in the same chamber as PECVD, and the filament was ignited in H_2 upon termination of film growth. Figure 3 reveals an important experimental observation. For the solid points, the *a*-Si:H was exposed to air between deposition and H treatment while at a temperature of 250°C. In this time a very thin oxide layer (< 10 Å) formed on the surface, presumably because the surface Si-H bonds are unstable at this temperature in the presence of oxygen and/or water vapor. The results of Fig. 3 show clearly that near-monolayer thicknesses of native oxide on *a*-Si:H act as an effective barrier to H. This result suggests that the filament-generated H does not enter the film freely through energetic penetration but rather via a chemical reaction that starts with H bonded at the surface. Apparently, the stronger Si-O

bond blocks this initial step. This supports the contention that H motion in *a*-Si:H occurs through Si-H bonding configurations.

Finally, the results in Fig. 3 show that any chemical equilibrium approaches to materials processing must be performed *in situ*. The implications of these results for interpreting H evolution are not yet fully clear. We would expect that an oxide layer would also serve as a barrier for exodiffusion of H, and this would be expected to affect H evolution experiments carried out extensively on *a*-Si:H.

IV. DISCUSSION AND SUMMARY

We will briefly compare our work to a very recent study of Jackson and Tsai that concentrated on SIMS measurements of *a*-Si posthydrogenated with microwave plasma-generated H.²⁰ The emphasis in Ref. 20 differs from ours in that PECVD *a*-Si:H was annealed to deplete the sample of the original H incorporated during growth, and the diffusion and trapping studies were performed from 320 to 450°C. These authors find that a concentration of $(0.8\text{--}2.0) \times 10^{20} \text{ cm}^{-3}$ H atoms are trapped at an energy deeper than 1.9 eV, and at least 30% of these trapping sites can be associated with dangling bonds.

In our case for *a*-Si:H at 250°C, Fig. 6 shows that at least ~ 10 vol % or $\sim 10^{21} \text{ cm}^{-3}$ H atoms can be deep trapped (depending on the filament conditions). Because our samples are optimum quality, these traps cannot include isolated dangling bond sites, which have been fully occupied in the growth process. It is possible that these traps represent clustered H_2^* pairs, but this would appear to be inconsistent with the proposal of Ref. 20 that such units act as traps with a binding energy of 1.5 eV/H. A possible explanation is that the binding energy may depend on the size of the H_2^* complex, with our higher binding energies representing larger complexes that may be present at the lower temperature of this study. Additional probes of the H-modified materials are required, however, to support such speculations. We conclude by emphasizing that a substantial number of tightly bound H atoms have been introduced that are unrelated to isolated dangling bond sites. These exhibit a 2000-cm^{-1} infrared stretching vibrational mode and must occur in pairs in order to maintain the low observed coordination defect density.¹² Such conclusions are consistent with recent negative- U models of H bonding in *a*-Si:H.²¹

In summary, we have applied a heated-filament technique for *in situ* hydrogenation that can be used controllably to increase the H chemical potential in *a*-Si:H for studies of H diffusion, trapping, and emission. Treatment of *a*-Si:H by atomic H generated by the heated filament has two primary advantages. First, the thermal H is not sufficiently energetic to damage the near surface of *a*-Si:H, and etching is kept to a very minimum. This is substantiated by the observation that near-monolayer levels of oxide on *a*-Si:H are not removed in the H treatment but rather act as an effective diffusion barrier. Second, the H treatment can be performed *in situ* with the *a*-Si:H at its deposition temperature ($\sim 250^\circ\text{C}$), mounted in the same configuration as conventional parallel-plate

PECVD. As a result, any improvements in bulk, surface, or interface properties of materials or devices can be adapted to existing processes.

We have applied this technique in conjunction with real-time spectroscopic ellipsometry to study H diffusion, trapping, and emission in optimum *a*-Si:H at $\sim 250^\circ\text{C}$ in order to understand the effects of H interaction with *a*-Si:H in the deposition environment. Interpretation of the processes occurring in the top 200 Å of the film, probed optically, is simplified since the dominant time scale for diffusion is faster than that for deep trapping, which in turn is much faster than emission. We find that the increase in bonded H in *a*-Si:H is limited by the capture of mobile H by deep traps. The rate at which additional H is deep trapped in the *a*-Si:H, given by the product of the capture rate coefficient and the concentration of mobile H, is $\sim 10^{-3} \text{ s}^{-1}$. Under our filament conditions, we estimate that the concentration of mobile H in the *a*-Si:H is on the order of 10^{20} cm^{-3} . About 85% of the $\sim 10^{21} \text{ cm}^{-3}$ H bonded into optimum *a*-Si:H (in addition to that already present from the growth process) exhibits an emission rate coefficient $< 2 \times 10^{-7} \text{ s}^{-1}$, suggesting that this H is trapped at a depth $> 2.0 \text{ eV}$. A smaller number of deep traps for the injected H, $\sim 2 \times 10^{20} \text{ cm}^{-3}$, appear to be present, having depths from 1.55 to 1.65 eV. In general, deep traps with trapping rate α become fully occupied in the growth process when the deposition rate

r is given by $r < \alpha x_c$, where x_c is the penetration depth of the H (see Fig. 5).

Finally, the shallow-trap-dominated diffusion coefficient within the top 200 Å of the film in the growth environment is $> 3 \times 10^{-15} \text{ cm}^2/\text{s}$, and probably higher. Using this result in simple H-equilibration arguments proposed earlier, growth behavior limited by the kinetics of H equilibration with the plasma would be obtained only at growth rates above 15 Å/s . Since *a*-Si:H films deposited at 15 Å/s are generally much poorer in electronic performance than conventional materials prepared at $\sim 2 \text{ Å/s}$, it is possible that slower surface processes (i.e., top few monolayers) during growth such as precursor surface diffusion or Si network formation and relaxation, rather than H equilibration, may ultimately limit the material performance under these conditions.

ACKNOWLEDGMENTS

This study was supported by the National Renewable Energy Laboratory under Subcontract No. XG-1-10063-10. Additional support to R.W.C. was also provided by the National Science Foundation under Grant No. DMR-8957159 and to Y.M.L. and C.R.W. by the Electric Power Research Institute. The authors also acknowledge the expert assistance of M. Frost of Evans East for SIMS analyses.

-
- ¹D. Das, H. Shirai, J. Hanna, and I. Shimizu, *Jpn. J. Appl. Phys.* **30**, L239 (1991).
- ²N. M. Johnson, C. E. Nebel, P. V. Santos, W. B. Jackson, R. A. Street, K. S. Stevens, and J. Walker, *Appl. Phys. Lett.* **59**, 1443 (1991).
- ³R. A. Street, *Phys. Rev. B* **43**, 2454 (1991).
- ⁴D. E. Carlson and C. W. Magee, *Appl. Phys. Lett.* **33**, 81 (1978).
- ⁵R. A. Street, C. C. Tsai, J. Kakalios, and W. B. Jackson, *Philos. Mag.* **B 56**, 305 (1987).
- ⁶J. Kakalios and W. B. Jackson, in *Amorphous Silicon and Related Materials*, edited by H. Fritzsche (World Scientific, Singapore, 1988), p. 207.
- ⁷V. Halpern, *Phys. Rev. Lett.* **67**, 611 (1991).
- ⁸A. E. Widmer, R. Fehlmann, and C. W. Magee, *J. Non-Cryst. Solids* **54**, 199 (1983).
- ⁹B. Abeles, L. Yang, D. Leta, and C. Majkrzak, *J. Non-Cryst. Solids* **97&98**, 353 (1987).
- ¹⁰P. V. Santos and W. B. Jackson, in *Amorphous Silicon Technology—1992*, edited by M. J. Thompson, Y. Hamakawa, P. G. LeComber, A. Madan, and E. Schiff, MRS Symposia Proceedings No. 258 (Materials Research Society, Pittsburgh, 1992), p. 425.
- ¹¹A. Asano, *Appl. Phys. Lett.* **56**, 53 (1990).
- ¹²Y. M. Li, I. An, M. Gunes, R. M. Dawson, R. W. Collins, and C. R. Wronski, in *Amorphous Silicon Technology—1992* (Ref. 10), p. 57.
- ¹³R. W. Collins, *Rev. Sci. Instrum.* **61**, 2029 (1990).
- ¹⁴Y. M. Li, I. An, H. V. Nguyen, C. R. Wronski, and R. W. Collins, *Phys. Rev. Lett.* **68**, 2814 (1992).
- ¹⁵R. W. Collins, in *Amorphous Silicon Technology*, edited by A. Madan, M. J. Thompson, P. C. Taylor, P. G. LeComber, and Y. Hamakawa, MRS Symposia Proceedings No. 118 (Materials Research Society, Pittsburgh, 1988), p. 19.
- ¹⁶K. Mui and F. W. Smith, *Phys. Rev. B* **38**, 10 623 (1988).
- ¹⁷A. R. Forouhi and I. Bloomer, *Phys. Rev. B* **34**, 7018 (1988).
- ¹⁸P. M. Richards, *J. Appl. Phys.* **70**, 4258 (1991).
- ¹⁹S. B. Zhang, W. B. Jackson, and D. J. Chadi, *Phys. Rev. Lett.* **65**, 2575 (1990).
- ²⁰W. B. Jackson and C. C. Tsai, *Phys. Rev. B* **45**, 6564 (1992).
- ²¹S. Zafar and E. A. Schiff, *Phys. Rev. B* **40**, 5235 (1990).